

Nuclear Modification Factors for Hadrons At Forward and Backward Rapidity in  
 Deuteron-Gold Collisions at  $\sqrt{s_{NN}} = 200 \text{ GeV}$

S.S. Adler,<sup>5</sup> S.A. Afanasev,<sup>20</sup> C.A. Adlara,<sup>10</sup> N.N. Aitanand,<sup>44</sup> Y. Akiba,<sup>21,40</sup> A. Al-Jamel,<sup>35</sup> J.A. Alexander,<sup>44</sup> K. Aoki,<sup>25</sup> L. Aphecetche,<sup>46</sup> R. Armandariz,<sup>35</sup> S.H. Aronson,<sup>5</sup> R. Averbeck,<sup>45</sup> T.C. Awes,<sup>36</sup> V. Babintsev,<sup>17</sup> A. Baldissari,<sup>11</sup> K.N. Barish,<sup>6</sup> P.D. Barnes,<sup>28</sup> B. Bassalleck,<sup>34</sup> S. Bathe,<sup>6,31</sup> S. Batsouli,<sup>10</sup> V. Baublis,<sup>39</sup> F. Bauer,<sup>6</sup> A. Bazilevsky,<sup>5,41</sup> S. Belikov,<sup>19,17</sup> M.T. Bjørndal,<sup>10</sup> J.G. Boissevain,<sup>28</sup> H. Borel,<sup>11</sup> M.L. Brooks,<sup>28</sup> D.S. Brown,<sup>35</sup> N. Brunner,<sup>34</sup> D. Bucher,<sup>31</sup> H. Buesching,<sup>5,31</sup> V. Bumazhnov,<sup>17</sup> G. Bunce,<sup>5,41</sup> J.M. Burward-Hoy,<sup>28,27</sup> S. Butsyk,<sup>45</sup> X. Camard,<sup>46</sup> P. Chand,<sup>4</sup> W.C. Chang,<sup>2</sup> S. Chemichenko,<sup>17</sup> C.Y. Chi,<sup>10</sup> J. Chiba,<sup>21</sup> M. Chiu,<sup>10</sup> I.J. Choi,<sup>53</sup> R.K. Choudhury,<sup>4</sup> T. Chujp,<sup>5</sup> V.C. Cianciolo,<sup>36</sup> Y. Cobigo,<sup>11</sup> B.A. Cole,<sup>10</sup> M.P. Comets,<sup>37</sup> P. Constantin,<sup>19</sup> M. Csanad,<sup>13</sup> T.C. Csongor,<sup>22</sup> J.P. Cussonneau,<sup>46</sup> D. d'Enterria,<sup>10</sup> K. Das,<sup>14</sup> G. David,<sup>5</sup> F. Deak,<sup>13</sup> H. Delagrange,<sup>46</sup> A. Denisov,<sup>17</sup> A. Deshpande,<sup>41</sup> E. J. Desmond,<sup>5</sup> A. Devismes,<sup>45</sup> O. Dietzsch,<sup>42</sup> J.L. Dachenberg,<sup>1</sup> O. D'rapier,<sup>26</sup> A. Drees,<sup>45</sup> A. Dunum,<sup>17</sup> D. Dutta,<sup>4</sup> V. Dzhordzhadze,<sup>47</sup> Y.V. Efremenko,<sup>36</sup> H. En'yo,<sup>40,41</sup> B. Espagnon,<sup>37</sup> S. Esuji,<sup>49</sup> D.E. Fields,<sup>34,41</sup> C. Finch,<sup>46</sup> F. Fleuret,<sup>26</sup> S.L. Fokin,<sup>24</sup> B.D. Fox,<sup>41</sup> Z. Fraenkel,<sup>52</sup> J.E. Frantz,<sup>10</sup> A. Franz,<sup>5</sup> A.D. Frawley,<sup>14</sup> Y. Fukao,<sup>25,40,41</sup> S.-Y. Fung,<sup>6</sup> S. Gadrat,<sup>29</sup> M. Germain,<sup>46</sup> A. Genn,<sup>47</sup> M. Gonin,<sup>26</sup> J. Gosset,<sup>11</sup> Y. Goto,<sup>40,41</sup> R. Granier de Cassagnac,<sup>26</sup> N. Gruau,<sup>19</sup> S.V. Gremee,<sup>50</sup> M. Grosse Perdekamp,<sup>18,41</sup> H. Gustafsson,<sup>30</sup> T. Hachiya,<sup>16</sup> J.S. Haggerty,<sup>5</sup> H. Hamagaki,<sup>8</sup> A.G. Hansen,<sup>28</sup> E.P. Hartouni,<sup>27</sup> M. Harvey,<sup>5</sup> K. Hasuko,<sup>40</sup> R. Hayano,<sup>8</sup> X. He,<sup>15</sup> M. Heiner,<sup>27</sup> T.K. Hemmick,<sup>45</sup> J.M. Heuser,<sup>40</sup> P. Hidas,<sup>22</sup> H. Heijima,<sup>18</sup> J.C. Hill,<sup>19</sup> R. Hobbs,<sup>34</sup> W. Holzmann,<sup>44</sup> K. Homma,<sup>16</sup> B. Hong,<sup>23</sup> A. Hoover,<sup>35</sup> T. Horaguchi,<sup>40,41,48</sup> T. Ichihara,<sup>40,41</sup> V.V. Ikonnikov,<sup>24</sup> K. Imai,<sup>25,40</sup> M. Inaba,<sup>49</sup> M. Inuzuka,<sup>8</sup> D. Isenhower,<sup>1</sup> L. Isenhower,<sup>1</sup> M. Ishihara,<sup>40</sup> M. Issah,<sup>44</sup> A. Isupov,<sup>20</sup> B.V. Jacak,<sup>45</sup> J. Jia,<sup>45</sup> O. Jinnouchi,<sup>40,41</sup> B.M. Johnson,<sup>5</sup> S.C. Johnson,<sup>27</sup> K.S. Joo,<sup>32</sup> D. Jouan,<sup>37</sup> F. Kajihara,<sup>8</sup> S. Kametani,<sup>8,51</sup> N. Kamihara,<sup>40,48</sup> M. Kaneta,<sup>41</sup> J.H. Kang,<sup>53</sup> K. Katou,<sup>51</sup> T. Kawabata,<sup>8</sup> A. Kazantsev,<sup>24</sup> S. Kelly,<sup>9,10</sup> B. Kachaturov,<sup>52</sup> A. Kanzadeev,<sup>39</sup> J. Kikuchi,<sup>51</sup> D.J. Kim,<sup>53</sup> E. Kim,<sup>43</sup> G.-B. Kim,<sup>26</sup> H.J. Kim,<sup>53</sup> E. Kinney,<sup>9</sup> A. Kiss,<sup>13</sup> E. Kistenev,<sup>5</sup> A. Kiyomichi,<sup>40</sup> C.Klein-Boesing,<sup>31</sup> H. Kobayashi,<sup>41</sup> L. Kochenda,<sup>39</sup> V. Kochetkov,<sup>17</sup> R. Kohara,<sup>16</sup> B. Komkov,<sup>39</sup> M. Konno,<sup>49</sup> D. Kotchetkov,<sup>6</sup> A. Kozlov,<sup>52</sup> P.J. Kroon,<sup>5</sup> C.H. Kuberg,<sup>1</sup> G.J. Kunde,<sup>28</sup> K. Kurita,<sup>40</sup> M.J. Kweon,<sup>23</sup> Y. Kwon,<sup>53</sup> G.S. Kyle,<sup>35</sup> R. Lacey,<sup>44</sup> J.G. Lapie,<sup>19</sup> Y. Le Borme,<sup>37</sup> A. Lebedev,<sup>19,24</sup> S. Leckey,<sup>45</sup> D.M. Lee,<sup>28</sup> M.J. Leitch,<sup>28</sup> M.A.L. Leite,<sup>42</sup> X.H. Li,<sup>6</sup> H. Lin,<sup>43</sup> A. Litvinenko,<sup>20</sup> M.X. Liu,<sup>28</sup> C.F. Maguire,<sup>50</sup> Y.I.M. Akdisi,<sup>5</sup> A.M. Alakhov,<sup>20</sup> V.I.M. Anko,<sup>24</sup> Y.M. Ao,<sup>38,40</sup> G.M. Martinez,<sup>46</sup> H.M. Asui,<sup>49</sup> F.M. Atathias,<sup>45</sup> T.M. Atsumoto,<sup>8,51</sup> M.C.M. Cain,<sup>1</sup> P.L.M. CG Aughey,<sup>28</sup> Y.M. Iake,<sup>49</sup> T.E. Miller,<sup>50</sup> A.M. Ilov,<sup>45</sup> S.M. Ioduszewski,<sup>5</sup> G.C. Mishra,<sup>15</sup> J.T.M. Itchell,<sup>5</sup> A.K.M. Ohanty,<sup>4</sup> D.P.M. Orrison,<sup>5</sup> J.M. Ooss,<sup>28</sup> D.M. Ukhopadhyay,<sup>52</sup> M.M. Uniruzzam an,<sup>6</sup> S.N. Agam Iya,<sup>21</sup> J.L. Nagle,<sup>9,10</sup> T.N. Nakamura,<sup>16</sup> J. Newby,<sup>47</sup> A.S. Nyanin,<sup>24</sup> J. Nystrand,<sup>30</sup> E.O. Brien,<sup>5</sup> C.A. Ogilvie,<sup>19</sup> H. Ohnishi,<sup>40</sup> I.D.O. Oja,<sup>3,50</sup> H.O. Kada,<sup>25,40</sup> K.O. Kada,<sup>40,41</sup> A.O. Skarsson,<sup>30</sup> I.O. Tterlund,<sup>30</sup> K.O. Yamada,<sup>8</sup> K.O. Zawa,<sup>8</sup> D. Pal,<sup>52</sup> A.P.T. Palubnek,<sup>28</sup> V. Pantuev,<sup>45</sup> V. Papavassiliou,<sup>35</sup> J. Park,<sup>43</sup> W.J. Park,<sup>23</sup> S.F. Pate,<sup>35</sup> H. Pei,<sup>19</sup> V. Penev,<sup>20</sup> J.-C. Peng,<sup>18</sup> H. Pereira,<sup>11</sup> V. Peresedov,<sup>20</sup> A. Pierson,<sup>34</sup> C.P. Pinenburg,<sup>5</sup> R.P. Pisani,<sup>5</sup> M.L. Purschke,<sup>5</sup> A.K. Purwar,<sup>45</sup> J.M. Qualls,<sup>1</sup> J. Rak,<sup>19</sup> I. Ravidovich,<sup>52</sup> K.F. Read,<sup>36,47</sup> M. Reuter,<sup>45</sup> K. Reygors,<sup>31</sup> V. Riabov,<sup>39</sup> Y. Riabov,<sup>39</sup> G. Roche,<sup>29</sup> A. Romana,<sup>26</sup> M. Rosati,<sup>19</sup> S.S.E. Rosendahl,<sup>30</sup> P. Rosnet,<sup>29</sup> V.L. Rykov,<sup>40</sup> S.S. Ryu,<sup>53</sup> N. Saito,<sup>25,40,41</sup> T. Sakaguchi,<sup>8,51</sup> S. Sakai,<sup>49</sup> V. Samsonov,<sup>39</sup> L. Sanfratello,<sup>34</sup> R. Santo,<sup>31</sup> H.D. Sato,<sup>25,40</sup> S. Sato,<sup>5,49</sup> S. Sawada,<sup>21</sup> Y. Schutz,<sup>46</sup> V. Semenov,<sup>17</sup> R. Seto,<sup>6</sup> T.K. Shea,<sup>5</sup> I. Shein,<sup>17</sup> T.A. Shibata,<sup>40,48</sup> K. Shigaki,<sup>16</sup> M. Shimomura,<sup>49</sup> A. Sickles,<sup>45</sup> C.L. Silva,<sup>42</sup> D. Silvermyr,<sup>28</sup> K.S. Sim,<sup>23</sup> A. Soldatov,<sup>17</sup> R.A. Soltz,<sup>27</sup> W.E. Sondheim,<sup>28</sup> S.P. Sorensen,<sup>47</sup> I.V. Sourikova,<sup>5</sup> F. Staley,<sup>11</sup> P.W. Stankus,<sup>36</sup> E. Stenlund,<sup>30</sup> M. Stepanov,<sup>35</sup> A. Ster,<sup>22</sup> S.P. Stoll,<sup>5</sup> T. Sugitate,<sup>16</sup> J.P. Sullivan,<sup>28</sup> S. Takagi,<sup>49</sup> E.M. Takagui,<sup>42</sup> A. Taketani,<sup>40,41</sup> K.H. Tanaka,<sup>21</sup> Y. Tanaka,<sup>33</sup> K. Tanida,<sup>40</sup> M.J. Tannenbaum,<sup>5</sup> A. Taranenko,<sup>44</sup> P. Tarjan,<sup>12</sup> T.L. Thomas,<sup>34</sup> M. Togawa,<sup>25,40</sup> J. Top,<sup>40</sup> H. Torii,<sup>25,41</sup> R.S. Towell,<sup>1</sup> V.-N. Tram,<sup>26</sup> I. Tsernuya,<sup>52</sup> Y. Tsuchimoto,<sup>16</sup> H. Tydesjö,<sup>30</sup> N. Tyurin,<sup>17</sup> T.J. Uam,<sup>32</sup> J. Velkovska,<sup>5</sup> M. Velkovsky,<sup>45</sup> V. Veszpremi,<sup>12</sup> A.A. Vinogradov,<sup>24</sup> M.A. Volkov,<sup>24</sup> E.V. Znuzdaev,<sup>39</sup> X.R. Wang,<sup>15</sup> Y.Watanabe,<sup>40,41</sup> S.N. White,<sup>5</sup> N. Willis,<sup>37</sup> F.K. Wohr,<sup>19</sup> C.L. Woody,<sup>5</sup> W.Xie,<sup>6</sup> A.Yanovich,<sup>17</sup> S.Yokkaichi,<sup>40,41</sup> G.R. Young,<sup>36</sup> I.E. Yushmanov,<sup>24</sup> W.A. Zajc,<sup>10</sup> C.Zhang,<sup>10</sup> S.Zhou,<sup>7</sup> J.Zimanyi,<sup>22</sup> L.Zolin,<sup>20</sup> X.Zong,<sup>19</sup> and H.W. van Hecke<sup>28</sup>

(PHENIX Collaboration)

<sup>1</sup> Abilene Christian University, Abilene, TX 79699, USA

<sup>2</sup> Institute of Physics, Academia Sinica, Taipei 11529, Taiwan

<sup>3</sup> Department of Physics, Banaras Hindu University, Varanasi 221005, India

<sup>4</sup>Bhabha Atomic Research Centre, Bombay 400 085, India  
<sup>5</sup>Brookhaven National Laboratory, Upton, NY 11973-5000, USA  
<sup>6</sup>University of California - Riverside, Riverside, CA 92521, USA  
<sup>7</sup>China Institute of Atomic Energy (CIAE), Beijing, People's Republic of China  
<sup>8</sup>Center for Nuclear Study, Graduate School of Science, University of Tokyo, 7-3-1 Hongo, Bunkyo, Tokyo 113-0033, Japan  
<sup>9</sup>University of Colorado, Boulder, CO 80309  
<sup>10</sup>Columbia University, New York, NY 10027 and Nevis Laboratories, Irvington, NY 10533, USA  
<sup>11</sup>Dapnia, CEA Saclay, F-91191, Gif-sur-Yvette, France  
<sup>12</sup>Dubrue University, H-4010 Debrecen, Egyetem ter 1, Hungary  
<sup>13</sup>ELTE, Eotvos Lorand University, H-1117 Budapest, Pfzamany P. s. 1/A, Hungary  
<sup>14</sup>Florida State University, Tallahassee, FL 32306, USA  
<sup>15</sup>Georgia State University, Atlanta, GA 30303, USA  
<sup>16</sup>Hiroshima University, Kagamiyama, Higashihiroshima 739-8526, Japan  
<sup>17</sup>Institute for High Energy Physics (IHEP), Protvino, Russia  
<sup>18</sup>University of Illinois at Urbana-Champaign, Urbana, IL 61801  
<sup>19</sup>Iowa State University, Ames, IA 50011, USA  
<sup>20</sup>Joint Institute for Nuclear Research, 141980 Dubna, Moscow Region, Russia  
<sup>21</sup>KEK, High Energy Accelerator Research Organization, Tsukuba-shi, Ibaraki-ken 305-0801, Japan  
<sup>22</sup>KFKI Research Institute for Particle and Nuclear Physics (RMKI), H-1525 Budapest 114, PO Box 49, Hungary  
<sup>23</sup>Korea University, Seoul, 136-701, Korea  
<sup>24</sup>Russian Research Center "Kurchatov Institute", Moscow, Russia  
<sup>25</sup>Kyoto University, Kyoto 606, Japan  
<sup>26</sup>Laboratoire Leprince-Ringuet, Ecole Polytechnique, CNRS-IN2P3, Route de Saclay, F-91128, Palaiseau, France  
<sup>27</sup>Lawrence Livermore National Laboratory, Livermore, CA 94550, USA  
<sup>28</sup>Los Alamos National Laboratory, Los Alamos, NM 87545, USA  
<sup>29</sup>LPC, Universite Blaise Pascal, CNRS-IN2P3, Clermont-Fd, 63177 Aubiere Cedex, France  
<sup>30</sup>Department of Physics, Lund University, Box 118, SE-221 00 Lund, Sweden  
<sup>31</sup>Institut für Kernphysik, University of Münster, D-48149 Münster, Germany  
<sup>32</sup>Myongji University, Yongin, Kyonggi-do 449-728, Korea  
<sup>33</sup>Nagasaki Institute of Applied Science, Nagasaki-shi, Nagasaki 851-0193, Japan  
<sup>34</sup>University of New Mexico, Albuquerque, NM 87131, USA  
<sup>35</sup>New Mexico State University, Las Cruces, NM 88003, USA  
<sup>36</sup>Oak Ridge National Laboratory, Oak Ridge, TN 37831, USA  
<sup>37</sup>IPN-Orsay, Université Paris Sud, CNRS-IN2P3, BP 1, F-91406, Orsay, France  
<sup>38</sup>Peking University, Beijing, People's Republic of China  
<sup>39</sup>PNPI, Petersburg Nuclear Physics Institute, Gatchina, Russia  
<sup>40</sup>RIKEN (The Institute of Physical and Chemical Research), Wako, Saitama 351-0198, JAPAN  
<sup>41</sup>RIKEN BNL Research Center, Brookhaven National Laboratory, Upton, NY 11973-5000, USA  
<sup>42</sup>Universidade de São Paulo, Instituto de Física, Caixa Postal 66318, São Paulo CEP 05315-970, Brazil  
<sup>43</sup>System Electronics Laboratory, Seoul National University, Seoul, South Korea  
<sup>44</sup>Chemistry Department, Stony Brook University, Stony Brook, SUNY, NY 11794-3400, USA  
<sup>45</sup>Department of Physics and Astronomy, Stony Brook University, SUNY, Stony Brook, NY 11794, USA  
<sup>46</sup>SUBATECH (Ecole des Mines de Nantes, CNRS-IN2P3, Université de Nantes) BP 20722 - 44307, Nantes, France  
<sup>47</sup>University of Tennessee, Knoxville, TN 37996, USA  
<sup>48</sup>Department of Physics, Tokyo Institute of Technology, Tokyo, 152-8551, Japan  
<sup>49</sup>Institute of Physics, University of Tsukuba, Tsukuba, Ibaraki 305, Japan  
<sup>50</sup>Vanderbilt University, Nashville, TN 37235, USA  
<sup>51</sup>Waseda University, Advanced Research Institute for Science and Engineering, 17 Kikui-cho, Shinjuku-ku, Tokyo 162-0044, Japan  
<sup>52</sup>Weizmann Institute, Rehovot 76100, Israel  
<sup>53</sup>Yonsei University, IAP, Seoul 120-749, Korea

(Dated: October 31, 2019)

We report on charged hadron production in deuteron-gold reactions at  $\frac{P_T}{\sqrt{s_{NN}}} = 200$  GeV. Our measurements in the deuteron-direction cover  $1.4 < \eta < 2.2$ , referred to as forward rapidity, and in the gold-direction  $2.0 < \eta < 1.4$ , referred to as backward rapidity, and a transverse momentum range  $p_T = 0.5 - 4.0$  GeV/c. We compare the relative yields for different deuteron-gold collision centrality classes. We observe a suppression relative to binary collision scaling at forward rapidity, sensitive to low momentum fraction (x) partons in the gold nucleus, and an enhancement at backward rapidity, sensitive to high momentum fraction partons in the gold nucleus.

PACS numbers: 25.75.Dw

Deep inelastic scattering of leptons on the proton revealed the proton's substructure of point-like parton con-

stituents [1]. This substructure, usually described quantitatively as Parton Distribution Functions, evolves as one probes the proton at shorter wavelength or equivalently higher momentum transfer,  $Q^2$ . Using the measured quark and antiquark distribution functions and the DGLAP and BFKL evolution equations [2], a strong increase in the gluon density is expected at high  $Q^2$  and small  $x$  (fraction of the proton momentum carried by the parton). Such an increase is indeed observed at HERA [3], suggesting that at sufficiently small  $x$ , gluons should overlap in space and time. This overlap should result in gluon fusion, and thus reduce the gluon density at low  $x$  and enhance it at larger  $x$ . This gluon fusion limits the achievable gluon density, leading to gluon saturation. This saturation is sometimes described as the formation of a Color Glass Condensate (CGC) [4]. Gluon saturation is expected to be a large effect in nuclei where the partons from different nucleons overlap as well. Suppression of low  $x$  partons in nuclei relative to nucleons has been experimentally observed and is referred to as nuclear shadowing [5]. However, this shadowing is often described in terms of modification of the leading-twist parton densities in nuclei [6].

In 2003 the Relativistic Heavy Ion Collider (RHIC) collided deuteron and gold nuclei at  $\sqrt{s_{NN}} = 200 \text{ GeV}$ . At this energy, most hadrons with  $p_T > 2.0 \text{ GeV}/c$  arise from parton-parton interactions and can be used as a probe of nuclear partonic structure. Hadrons with  $p_T > 2.0 \text{ GeV}/c$  at forward rapidity  $1.4 < \eta < 2.2$  are sensitive to low  $x$  partons in the gold nucleus  $0.001 < x < 0.03$ . Hadrons at backward rapidity  $-2.0 < \eta < -1.4$  are sensitive to high  $x$  partons in the gold nucleus  $0.04 < x < 0.5$ . It has been predicted that gluon saturation at small  $x$  will suppress hadronic yields at forward rapidity [7] with the transverse momentum scale for the onset of the gluon saturation set by  $Q_s^2 [\text{GeV}^2] = 0.13 N_{\text{coll}} e^y$  [8] for  $d + \text{Au}$  collisions at RHIC. Here  $0.3$  is determined from HERA data [9] and  $N_{\text{coll}}$  is the number of nucleon-nucleon inelastic collisions. Thus, for central collisions and within our forward rapidity coverage  $Q_s^2$  is expected to be of order  $2-4 \text{ GeV}^2$  and may have observable consequences. Other hadron production mechanisms, such as quark recombination [10], can also result in an effective suppression in the forward rapidity region.

Results on charged hadron yields at forward rapidity from the BRAHMS experiment have shown a suppression of the yield of hadrons in central, compared to peripheral,  $d + \text{Au}$  collisions [11]. At mid-rapidity, PHENIX has reported a modest enhancement of the yield of hadrons with  $p_T > 1.5 \text{ GeV}/c$  [12]. This enhancement, generally referred to as the "Cronin effect" is often ascribed to initial state scattering of the parton traversing the nucleus prior to the high  $Q^2$  scattering [13]. At backward rapidities (large  $x$ ), anti-shadowing and other effects of the surrounding nuclear medium (e.g. the EMC effect) [14] may compete, making predictions challenging.

It is important to note that in the transverse momentum range of this measurement,  $0.5 < p_T < 4.0 \text{ GeV}/c$ , hadron production is also sensitive to soft physics phenomena which are determined by coherent hadron-hadron interactions. In  $p + A$  reactions at lower energies soft hadron production shifts from forward to backward rapidity, with a larger shift for larger nuclear targets. This can be understood as rapidity exchange between incident and target nucleons. Thus, at low  $p_T$  one may observe an increase (decrease) in hadron yields at backward (forward) rapidity which is not necessarily a reflection of changes at the partonic structure level.

In this Letter, we present results from the PHENIX experiment [15] on the ratio of hadron yields at forward and backward pseudorapidity for different centrality classes of  $d + \text{Au}$  collisions. PHENIX has two spectrometers designed for measuring muon production over the pseudorapidity range  $-2.2 < \eta < -1.2$  (backward spectrometer) and  $1.2 < \eta < 2.4$  (forward spectrometer) [15]. The spectrometers start with a thick hadron absorber comprised of 19 cm of brass and 60 cm of low-carbon steel between the collision point and active detectors along the beam axis, primarily to reduce hadronic background for muon measurements [16]. After this material, the Muon Tracker (MuTr) detector, consisting of three stations of cathode strip chambers, tracks charged particles in a magnetic field. The momentum resolution is 5% (for typical momenta in this analysis) and the absolute scale is known to better than 1%.

Following the muon magnet backplate (30 (20) cm of steel in the forward (backward) spectrometer) there is a Muon Identifier (MuID) detector. The MuID consists of five layers of planar drift tubes interleaved with layers of steel for further hadron absorption (10 cm thick in the first two layers and 20 cm thick for the remaining layers). The layers are numbered 0-4, with 4 being the most downstream. The MuID is used to separate muons from hadrons and provide triggering capabilities.

Although these spectrometers were designed to detect muons, they can also be used to measure charged hadrons. Both muons and hadrons lose energy when passing through material via ionization energy loss. Hadrons also undergo strong nuclear interactions which substantially reduce their ability to penetrate through the spectrometer.

We have two independent methods of measuring hadrons. The first method is via the identification of hadrons which penetrate part way through the MuID, referred to as "punch-through hadrons." The second method is via muons from light mesons ( $K$  which decay before interacting in the absorber material). By measuring these decay muons, we can reconstruct the yield of their parent light mesons. In both of these methods the absolute yield of hadrons is difficult to determine due to uncertainties in the punch-through and decay probabilities. However, this small probability is independent of

d + Au collision centrality, and thus not knowing the absolute yields does not affect the precision of measured ratios of hadron yields between the different classes of events.

The punch-through hadron identification is achieved by studying particles that stop somewhere within the MuID before the last layer. For muons penetrating up to layer 2 and 3 we expect the average momentum measured in the MuTr of  $p = 1.0$  GeV/c and  $p = 1.2$  GeV/c, respectively. The reconstructed momentum distributions for particles stopping in layers 2 and 3 of the MuID are shown in Figure 1. In addition to the expected muon peaks, there is a broad distribution extending to higher momentum which is the result of punch-through hadrons. These hadrons also suffer ionization energy loss up to the relevant layer and then suffer an inelastic collision in the MuID steel and do not penetrate further. We thus select a clean sample of hadrons by demanding that a track stop in MuID layer 2 or 3 and have momentum more than 3 away from the muon peaks. Muon contamination in our sample is estimated from simulations to be less than 5%.

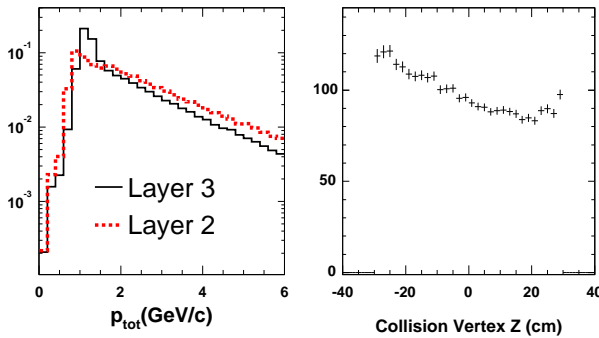


FIG. 1: (color online). (left) The total momentum  $p_{\text{tot}}$  measured in the MuTr without energy loss correction of all charged tracks penetrating to MuID layers 2 (grey) and 3 (black). (right) Collision vertex distribution for events with muons at forward rapidity, corrected for the minimum bias collision vertex distribution.

Another source of background for the punch-through hadrons is secondary particles produced from hadronic showering in the absorber. This background is reduced by requiring that the track point back to the primary collision vertex, as determined from the Beam-Beam Counter (BBC). The background from secondary particles varies as a function of  $p_{\text{t}}$  and is typically 1–5% of the signal based on simulations. We also apply acceptance cuts  $2.0 < \eta < 1.4$  and  $1.4 < \eta < 2.2$  in order to reduce background at small angles.

Some hadrons will decay into muons before the absorber, and the decay muons are then measured by the muon spectrometers. Muons can result from many sources including decays of  $\pi$ ,  $K$ ,  $D$  mesons, and  $J/\psi$ . These particles have a finite decay probability  $P_{\text{decay}}$  before they reach the absorber

$$P_{\text{decay}}(p; L) = 1 - e^{-\frac{L \cdot m}{p}} \quad (1)$$

where  $L = 41$  cm, is the distance from the collision vertex to the absorber;  $p$ ,  $m$  and  $L$  are the momentum, mass and proper lifetime of the parent particle.

Thus, collisions that occur far from the absorber will be more likely to produce muons from light meson decays than those that occur close to the absorber. Charm hadrons, however, due to their very short proper decay lengths,  $e^{-\frac{L \cdot m}{p}} \approx 1$ , will have minimal collision vertex dependence. The right panel of Figure 1 shows the collision vertex distribution from events in which muons are detected at forward rapidity, corrected for the minimum bias collision vertex distribution. The large vertex dependence indicates a significant fraction of the muons are from pion and kaon decay. Using this distribution, we can separate the muons from pion and kaon decay from other contributions. It should be noted that the measured muon  $p_{\text{t}}$  is approximately 15% lower on average than the parent hadron  $p_{\text{t}}$ .

The data set for this analysis was collected under two different trigger conditions. We recorded  $67 \times 10^6$  minimum bias triggers which required at least one hit in both the PHENIX forward  $3.0 < \eta < 3.9$  and backward

$3.9 < \eta < 3.0$  Beam-Beam Counters (BBC) and a reconstructed vertex position within  $|z| < 30$  cm along the beam axis. The minimum bias trigger accepts 88–4% of all inelastic d + Au collisions [12]. The second data set, sampling  $5.3 \times 10^6$  minimum bias events, was collected with the MuID trigger which requires at least one track penetrating the first four layers of the MuID.

We divide these events into four centrality classes based on the number of particle hits in the backward BBC counter covering  $3.9 < \eta < 3.0$ . Using a Glauber model [12] and simulation of the BBC, we determine the average number of binary collisions in each centrality class. The classes are categorized as follows: 60–88% ( $n_{\text{coll}} = 3.1 \pm 0.3$ ), 40–60% ( $n_{\text{coll}} = 7.0 \pm 0.6$ ), 20–40% ( $n_{\text{coll}} = 10.6 \pm 0.7$ ), and 0–20% ( $n_{\text{coll}} = 15.4 \pm 1.0$ ).

There is a correlation between having a particular physics process (for example the production of a high  $p_{\text{t}}$  hadron) and the BBC response. The BBC coverage in pseudorapidity is well separated from the muon spectrometers so the correlation is not predominantly due to jet fragmentation, but rather an underlying event correlation. We have studied this effect in detail using proton-proton and d + Au data, and in simulations, and have accounted for this correlation bias. The bias correction factors we apply range from 0–7% depending on the centrality category and the physics process. The systematic errors on these corrections are less than 4%.

The nuclear modification factor  $R_{\text{cp}}$  is defined as the ratio of the particle yield in central collisions to the particle yield in peripheral collisions, each normalized by

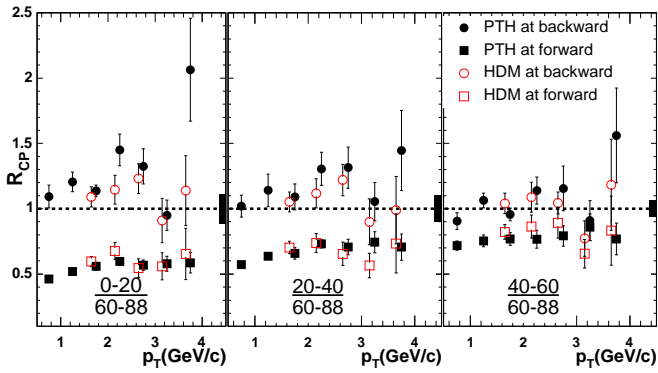


FIG. 2: (color online).  $R_{cp}$  as a function of  $p_T$  at forward rapidity (squares) and backward rapidity (circles) for different centrality classes.

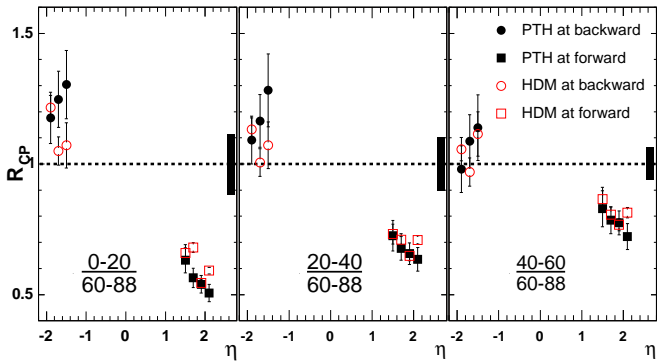


FIG. 3: (color online).  $R_{cp}$  as a function of  $\eta$  for  $1.5 < p_T < 4.0$  GeV/c for different centrality classes.

the average number of nucleon-nucleon binary collisions ( $\langle N_{coll} \rangle$ ):

$$R_{cp} = \frac{h \frac{dN}{dp_T} \text{Central}_{i=N_{coll}^{\text{central}}}^{i=N_{coll}^{\text{central}}} i}{h \frac{dN}{dp_T} \text{Peripheral}_{i=N_{coll}^{\text{peripheral}}}^{i=N_{coll}^{\text{peripheral}}} i} \quad (2)$$

The hadron  $R_{cp}$ , using the most peripheral centrality class (60–88%) for normalization, is shown in Figure 2 as a function of  $p_T$  at forward and backward rapidities. The results from the punch-through hadron (PTH) and hadron decay muon (HDM) techniques are both shown and are in quite good agreement. We also show the results integrated over  $1.5 < p_T < 4.0$  GeV/c as a function of pseudorapidity in Figure 3.

There are two types of systematic uncertainties in our analysis. Common systematic errors which move all data points up and down together include the error on  $\frac{N_{coll}^{\text{central}}}{N_{coll}^{\text{peripheral}}}$  (10.8% for the most central bin), the centrality bias correction factors (4%), and the centrality-dependent tracking efficiency (4%) determined by embedding Monte Carlo particles in real data. Common systematic errors are shown as a black bar. Point-to-

point systematic errors result from sensitivities to analysis cuts and are 5–10%. They are added in quadrature with the statistical errors and shown as error bars.

It is notable that our two measurement methods have different sensitivity to different hadrons. The particle composition ( $=K/p$  ratio) we measure is modified relative to the particle composition at the collision vertex due to species-dependent nuclear interaction cross-sections affecting the punch-through hadrons and due to species-dependent decay lifetimes affecting the hadron decay muons. Both effects enhance the kaon contribution to our  $R_{cp}$  measurements. The uncertainty on our charged hadron  $R_{cp}$  values introduced by this effect is estimated to be less than 4% by calculating the difference between the kaon  $R_{cp}$  and inclusive charged particle  $R_{cp}$  determined by PHENIX at mid-rapidity [17].

We observe that  $R_{cp}$  shows a suppression at forward rapidity that is largest for the most central events. The opposite trend is observed at backward rapidity where  $R_{cp}$  shows an enhancement that is also largest for the most central events. We observe a weak  $p_T$  dependence with slightly smaller  $R_{cp}$  values at lower  $p_T$ . We observe a clear pseudorapidity dependence at forward rapidity with  $R_{cp}$  dropping further at larger values. Within our current uncertainties we are unable to discern any pseudorapidity dependence at backward rapidity.

In Figure 4 we compare results from the BRAHMS experiment [11] with our results at forward rapidity. The PHENIX data and the BRAHMS data are in agreement within systematic uncertainties.

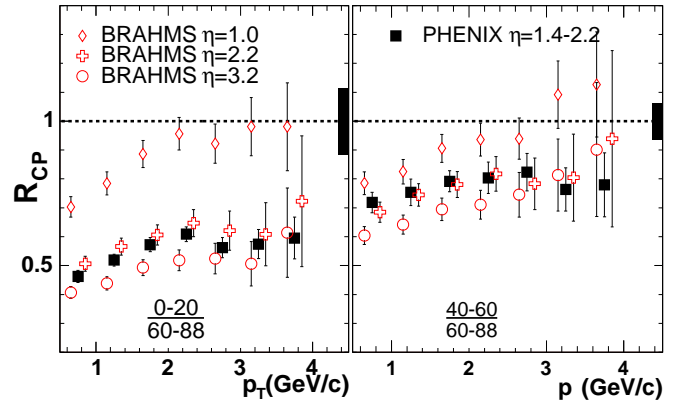


FIG. 4: (color online). PHENIX  $R_{cp}$  as a function of  $p_T$  at forward rapidities shown as the average of the two methods. Note that the BRAHMS results are for negative hadrons at  $\eta = 2.2; 3.2$  and their centrality ranges (0–20% = 60–80% and 30–50% = 60–80%) are somewhat different from ours.

The suppression of hadron yields relative to binary collision scaling at forward rapidity is expected from initial state nuclear effects. However, detailed comparisons with various theoretical approaches is necessary in order to discriminate between different models. In particular the lack of a strong  $p_T$  dependence at both forward and

backward rapidities must be understood as the physics processes transition from "soft" to "hard" physics scales.

To summarize, we observe a suppression in hadron yields relative to binary collision scaling at forward rapidities and an enhancement at backward rapidity for central relative to peripheral  $p_{\text{miss}}$   $\sqrt{s_{\text{NN}}} = 200 \text{ GeV}$ . The forward rapidity suppression is in qualitative agreement with the expectation of shadowing and saturation effects in the small  $x$  region in the gold nucleus. However, other physics effects must also be considered in understanding the full  $p_{\text{T}}$  and  $x$  dependence. The source of the backward rapidity enhancement, and the possible contribution of anti-shadowing of large  $x$  partons, has yet to be understood.

We thank the staff of the Collider-Accelerator and Physics Departments at BNL for their vital contributions. We acknowledge support from the Department of Energy and NSF (USA), MEXT and JSPS (Japan), CNPq and FAPESP (Brazil), NSFC (China), IN2P3/CNRS, CEA, and ARMINES (France), BMBF, DAAD, and AvH (Germany), OTKA (Hungary), DAE and DST (India), ISF (Israel), KRF and CHEP (Korea), RMIST, RAS, and RMAE (Russia), VR and KAW (Sweden), US-DOE for the FSU, US-Hungarian NSF-OTKA-MTA, and US-Israel BSF.

---

PHENIX Spokesperson: [zaj@nevis.columbia.edu](mailto:zaj@nevis.columbia.edu)

- [1] J. D. Bjorken and E. A. Paschos, *Phys. Rev.* **185**, 1975 (1969).
- [2] G. A. Litarelli and G. Parisi, *Nucl. Phys. B* **126**, 298 (1977); Y. L. Dokshitzer, *Sov. Phys. JETP* **46**, 641 (1977); V. N. Gribov and L. N. Lipatov, *Sov. J. Nucl. Phys.* **15**, 438 (1972).
- [3] H. Abramowicz and A. C. Caldwell, *Rev. Mod. Phys.* **71**, 1275 (1999).
- [4] L. M. Cullen and R. Venugopalan, *Phys. Rev. D* **49**, 2233 (1994); *Phys. Rev. D* **49**, 3352 (1994).
- [5] J. Ashman et al., *Phys. Lett. B* **202**, 603 (1988).
- [6] V. Guzey, M. Strikman and W. Vogelsang, arXiv:hep-ph/0407201.
- [7] A. Dumitru and J. Jalilian-Marian, *Phys. Lett. B* **547**, 15 (2002); F. G.олос and J. Jalilian-Marian, *Phys. Rev. D* **66**, 014021 (2002).
- [8] D. Kharzeev, Y. V. Kovchegov and K. Tuchin, arXiv:hep-ph/0405045.
- [9] K. Golec-Biernat and M. Wustho, *Phys. Rev. D* **59**, 014017 (1999); K. Golec-Biernat and M. Wustho, *Phys. Rev. D* **60**, 114023 (1999).
- [10] R. Hwa, C. B. Yang, R. J. Fries, arXiv:nucl-th/0410111.
- [11] I. Arsene et al., *Phys. Lett. B* **595**, 209 (2004).
- [12] S. S. Adler et al., *Phys. Rev. Lett.* **91**, 072303 (2003).
- [13] D. Antreasyan et al., *Phys. Rev. D* **19**, 764 (1979).
- [14] M. Amedeo, *Phys. Repts.* **240**, 301 (1994).
- [15] K. Adcox et al., *Nucl. Instrum. Methods A* **499**, 469 (2003) and references therein.
- [16] S. H. Amnon et al., *Nucl. Instrum. Methods A* **449**, 480-488 (2003).
- [17] F. M. Atathias et al., *J. Phys. G* **30**, S1113 (2004).